LA-UR-23-20189

Approved for public release; distribution is unlimited.

Title:	Plutonium Oxidation State Distribution under WIPP Relevant Conditions
Author(s):	Beam, Jeremiah Cooper
Intended for:	Report
Issued:	2025-05-27 (rev.2)

Los Alamos
NATIONAL LABORATORY







Los Alamos National Laboratory, an affirmative action/equal opportunity employer, is operated by Triad National Security, LLC for the National Nuclear Security Administration of U.S. Department of Energy under contract 89233218CNA000001. By approving this article, the publisher recognizes that the U.S. Government retains nonexclusive, royalty-free license to publish or reproduce the published form of this contribution, or to allow others to do so, for U.S. Government purposes. Los Alamos National Laboratory requests that the publisher identify this article as work performed under the auspices of the U.S. Department of Energy. Los Alamos National Laboratory strongly supports academic freedom and a researcher's right to publish; as an institution, however, the Laboratory does not endorse the viewpoint of a publication or guarantee its technical correctness.

ERRATA SHEET

The Following Corrections and Clarifications Apply to: LCO-ACP-31 Revision 1, *Plutonium Oxidation State Distribution under WIPP Relevant Conditions*

Document Number: LCO-ACP-31

Revision: 1

Original Document Issuance Date: January 19, 2023

Applicable Change(s): The following table identifies the corrections to LCO-ACP-31 Revision 1:

Page	Original Text	Correction
16	"Both Pu-239 and Pu-242 were used in these experiments. Both isotopes were procured from…"	"Pu-239 was used in these experiments. It was procured from…"
18	Last 7 lines in Table 3 reference Pu242 samples	Disregard Pu242 lines in Table 3
22	Table 5 contains 6 lines that reference Pu242 samples	Disregard Pu242 lines in Table 5
25	Table 6 contains 4 lines that reference Pu242 samples	Disregard Pu242 lines in Table 6

Reason for change: Samples containing Pu-242 should not have been included in this report, since they were generated by a postdoc who was not trained to the LANL-CO QA program at the time.

NOTE 1: This Errata Sheet must remain with LCO-ACP-31 Revision 1, *Plutonium Oxidation State Distribution under WIPP Relevant Conditions*

NOTE 2: Apart from this Errata Sheet, no other changes were made to LCO-ACP-31 Revision 1, *Plutonium Oxidation State Distribution under WIPP Relevant Conditions*.

NOTE 3: For all future citations of this work, please refer to the current revision of LCO-ACP-38, *Plutonium Oxidation State Distribution in the Presence of WIPP-Relevant Organics and Iron Corrosion Products.*

NOTICE: The current controlled version of this document is on the LCODocs website (http://lcodocs.lanl.gov/). A printed copy of the document may not be the current version.

LOS ALAMOS NATIONAL LABORATORY
CARLSBAD OPERATIONS

LCO-ACP-31, Rev 1

Plutonium Oxidation State Distribution under WIPP Relevant Conditions

Effective Date: 1-19-2023

Originator:

Jeremiah Beam, LANL-CO ACRSP — 1/19/23 Date

Reviewed by:

Ugras Kaplan, LANL-CO ACRSP — 01/19/23 Date

Approved by:

Jeremiah Beam, LANL-CO ACRSP Team Leader — 1/19/23 Date

Priscilla Yanez, LANL-CO Quality Assurance Manager — 1/19/2023 Date

Douglas Weaver, WIPP/RSO Program Director — 1-19-2023 Date

Revision Number	Effective Date	Description of Revision
0	1/9/2023	Initial Release
1	1/19/2023	Incorporated comments from Department of Energy and Sandia National Laboratories

Executive Summary

The oxidation state of plutonium in the Waste Isolation Pilot Plant (WIPP) environment has been a topic of interest since the initial compliance certification application. Plutonium (Pu) was initially expected to be present primarily as Pu(IV), but since the presence of Pu(III) could not be ruled out, it was also included in performance assessment (PA) calculations. The redox of the other variant actinides, uranium (U) and neptunium (Np), are also coupled to the plutonium redox. This led to a position in performance assessment calculations that is commonly referred to as "50/50". In which half of the PA realizations assume solubility is dominated by the low oxidation state [U(IV), Np(IV), Pu(III)] and the other half assume solubility is dominated by the higher oxidation state [U(VI), Np(V), Pu(IV)].

Recently, a joint group of WIPP project participants from Los Alamos National Laboratory (LANL), Sandia National Laboratories (SNL), and the Department of Energy's Carlsbad Field Office (DOE-CBFO) agreed on a new path forward for the oxidation state model in PA which will decouple the redox active actinides and will instead consider their redox as a function of E_h. This will take the current binary approach and turn it into a system with four possible redox states.

This work builds on all previous plutonium experiments and attempts to study the solubility of plutonium under a range of expected WIPP conditions, as well as determine the oxidation state of the solid phase which will control the solubility. Thermodynamic modeling of this system will be used to assess the relative effects of hydrogen overpressures that may be present due to anoxic corrosion of steel containers, and radiolysis of brine from the decay of waste materials.

X-ray Absorption Near-Edge Spectroscopy (XANES) analysis using Linear Combination Fitting (LCF) of Pu(III) and Pu(IV) standard spectra indicate that under all conditions expected in WIPP that Pu(IV) solids will dominate, in contrast to the United State Environmental Protection Agency's (US EPA) position that Pu(III) solids will dominate. A summary of the data collected in this report will be submitted to SNL as part of a parameter update report which will outline the changes to the oxidation state model for the 2024 Compliance Recertification Application (CRA-2024).

Table of Contents

List of Figures..... 5

List of Tables..... 6

References..... 7

Acronyms..... 9

Introduction..... 12

Experimental..... 15

Results and Discussion..... 18

Conclusion..... 26

List of Figures

Figure 1. UV-vis spectrum of Pu(III) stock solution in high purity water…… 16

Figure 2. Solubility of plutonium as a function of pC_{H+}…… 19

Figure 3. Pourbaix diagram of iron under WIPP relevant conditions. Diagram was calculated using the Thermochimie SIT database…… 21

Figure 4. Comparison of Pu speciation a) including solids, and b) only aqueous species under 1 atm H_2 overpressure. Diagrams were calculated using the Thermochimie SIT database…… 23

Figure 5. Pourbaix diagrams of plutonium ([Pu] = $1.2x10^{-7}$ M) solids in GWB under a) 1 atm and b) 80 atm H_2 overpressures. Diagrams were calculated using the Thermochimie SIT database……..23

Figure 6. XANES spectra of Pu(III/IV/VI) species…… 24

Figure 7. Sample LCF showing fit to Pu(III/IV) spectra and the residual of the fit…….. 25

List of Tables

Table 1. Composition of brines used in plutonium solubility experiments…… 15

Table 2. Concentration of species in WIPP brines used in Pu solubility experiments……. 15

Table 3. Experimental matrix for plutonium oxidation state studies……..18

Table 4. pC_{H+} values at each sampling……20

Table 5. ORP measurements, and E_h corrections for Pu solubility experiments. ORP measurements are corrected to E_h by adding the half-cell potential of Ag/AgCl reference (+209 mV at 25 °C)……..22

Table 6. LCF analysis of Pu(III)/Pu(IV) XANES spectra…… 25

References

Al Mahamid, I.; Becraft, K.A.; Hakem, N.L; Gatti, R.C.; Nitsche, H. Stability of Various Plutonium Valence States in the Presence of NTA and EDTA. **1996.** *Radiochimica Acta*. 74, 129.

Arumugam, K.; Burton, N.A. Disproportionation of the Uranyl(V) Coordination Complexes in Aqueous Solution through Outer-Sphere Electron Transfer. **2021.** *Inorganic Chemistry.* 60 (24), 18832.

Beam, J.C. Memo to Anderson Ward. Subject: Justification for Updating OXSTAT Parameter in Performance Assessment Calculations. **2022.** LA-UR-22-30617.

Brush, L. Test Plan for Laboratory and Modeling Studies of Radionuclide Chemistry for the Waste Isolation Pilot Plant SAND90-0266. **1990**. Sandia National Laboratories, Albuquerque, NM.

Büppelmann, K.; Magirius, S.; Lierse, Ch.; Kim, J.I. Radiolytic Oxidation of Americium(III) to Americium(V) and Plutonium(IV) to Plutonium(VI) in Saline Solution. **1986.** Journal of the Less-Common Metals. 122, 329.

Clark, D.L.; Hobart, D.E.; Neu, M.P. Actinide Carbonato Complexes and Their Importance in Actinide Environmental Chemistry. **1995.** *Chemical Reviews.* 95, 25.

Conradson, S.D.; Abney, K.D.; Begg, B.D.; Brady, E.D.; Clark, D.L.; den Auwer, C.; Ding, M.; Dorhout, P.K.; Espinosa-Faller, F.J.; Gordon, P.L.; Haire, R.G.; Hess, N.J.; Hess, R.F.; Keogh, D.W.; Lander, G.H.; Lupinetti, A.J.; Morales, L.A.; Neu, M.P.; Palmer, P.D.; Paviet-Hartmann, P.; Reilly, S.D.; Runde, W.H.; Tait, C.D.; Veirs, D.K.; Wastin F. Higher Order Speciation Effects on Plutonium L_3 X-ray Absorption Near Edge Spectra. **2004**. *Inorganic Chemistry*. 43, 116.

Felmy, A.R.; Rai, D.; Schramke, J.A.; Ryan, J.L. The Solubility of Plutonium Hydroxide in Dilute Solution and High-Ionic-Strength Chloride Brines. **1989.** Radiochimica Acta. 48, 29.

Giffaut, E.; Grivé, M.; Blanc, P.; Vieillard, P.; Colàs, E.; Gaihanou, H.; Gaboreau, S.; Marty, N.; Madé, B.; Duro, L. Andra thermodynamic database for performance assessment: ThermoChimie. **2014.** *Applied Geochemistry*. 49, 225.

Grivé, M.; Duro, L.; Colàs, E.; Giffaut, E. Thermodynamic data selection applied to radionuclides and chemotoxic elements: an overview of the ThermoChimie-TDB. **2015**. *Applied Geochemistry*. 55, 85.

Hansen, C.W. Review of Conceptual Models for the Additional Panels Performance Assessment. **2021.** ERMS 575523. Carlsbad, NM. Sandia National Laboratories.

Hobart, D.E. Actinides in the Environment. **1990.** Proceedings of the Robert A. Welch Foundation Conference on Chemical Research XXXIV. Houston, TX.

Katz, J.J.; Seaborg, G.T.; Morss, L.R. The Chemistry of the Actinide Elements, Second Edition. **1986.** Chapman and Hall, New York.

Moog, H.C.; Bok, F.; Marquardt, C.M.; Brendler, V. Disposal of nuclear waste in host rock formations featuring high-saline solutions – Implementation of a thermodynamic reference database (THEREDA). **2015.** *Applied Geochemistry*. 55, 72.

Rai, D.; Gorby, Y.A.; Fredrickson, J.K.; Moore, D.A.; Yui, M. Reductive Dissolution of PuO_2(am): The Effect of Fe(II) and Hydroquinone. **2002.** *J. Solution Chemistry*. 31, 6, 433.

Ravel. B.; Newville, M. ATHENA, ARTEMIS, HEPHAESTUS: data analysis for X-ray absorption spectroscopy using IFEFFIT. **2010**. *J. Synchrotron Radiation*. 12, 4.

Reed, D.T.; Aase, S.B.; Wygman, D.; Banaszak, J.E. The Reduction of Np(VI) and Pu(VI) by Organic Chelating Agents. **2003.** *Radiochimica Acta.* 82, 109.

Reed, D.T.; Lucchini, J.F.; Aase, S.B.; Kropf, A.J. Reduction of plutonium(VI) in brine under subsurface conditions. **2006**. *Radiochimica Acta*. 94, 591.

Schramke, J.A.; Santillan, E.F.U.; Peake, R.T. Plutonium oxidation states in the Waste Isolation Pilot Plant repository. **2020.** *Applied Geochemistry*. 116, 104561.

Sebin, J.; Ortego, J.D. Chemistry of uranium (V). **1969**. *Chemical Reviews.* 69, 5, 657.

U.S. DOE 2004. Title 40 CFR Part 191 Compliance Recertification Application for Waste Isolation Pilot Plant (March). Carlsbad, NM: Carlsbad Field office. DOE/WIPP 2004-3231

U.S. DOE 2009. Title 40 CFR Part 191 Compliance Recertification Application for Waste Isolation Pilot Plant (March). Carlsbad, NM: Carlsbad Field office. DOE/WIPP 2009-342

U.S. DOE 2014. Title 40 CFR Part 191 Compliance Recertification Application for Waste Isolation Pilot Plant (March). Carlsbad, NM: Carlsbad Field Office. DOE/WIPP 2014-3503

U.S. DOE 2019. Title 40 CFR Part 191 Compliance Recertification Application for Waste Isolation Pilot Plant (March). Carlsbad, NM: Carlsbad Field Office.

U.S. EPA 2013. Field Measurement of Oxidation-Reduction Potential (ORP). Athens, Georgia.

Van Soest, G.D. Performance Assessment Inventory Report - 2018. **2018**. LANL-CO. LA-UR-18-31882.

Weiner, R.W.; Hobart, D.E.; Tait, C.D.; Clark, D.L. Analysis of Actinide Oxidation States in the WIPP. **1996**. Sandia National Laboratories. ERMS 523410.

Acronyms and Definitions

AgCl	Silver(I) chloride
Am(III)	Americium in the +3 oxidation state, also written Am^{3+}
APS	Advanced Photon Source
atm	Atmospheres
BGE	Bundesgesellschaft Für Endlagerung (Federal Company for Radioactive Waste Disposal)
°C	Degrees Celsius or Centigrade
CBFO	Carlsbad Field Office
CCA	Compliance Certification Application
Cm(III)	Curium in the +3 oxidation state, also written Cm^{3+}
CRA	Compliance Recertification Application
DBR	Direct Brine Release
DOE	(United States) Department of Energy
E_h	oxidation-reduction potential (vs. Standard Hydrogen Electrode)
EDTA	Ethylenediaminetetraactetic acid
EPA	(United States) Environmental Protection Agency
ERDA-6	Energy Research and Development Administration Well 6
eV	Electron volt
Fe^0	Iron metal
Fe^{2+}	Ferrous iron, dissolved iron in the +2 oxidation state
Fe_3O_4	Magnetite
FeS_2	Pyrite
GWB	Generic Weep Brine
ICP-MS	Inductively Coupled Plasma Mass Spectrometry
L	Liter

LANL	Los Alamos National Laboratory
LCF	Linear Combination Fitting
K	Kelvin
kDa	Kilodalton
M	Molarity, moles of solute per liter of solvent
mV	Millivolt
NEA	Nuclear Energy Agency
Np(IV)	Neptunium in the +4 oxidation state, also written Np^{4+}
Np(V)	Neptunium in the +5 oxidation state, also written NpO_2^+
ORP	Oxidation-Reduction Potential
PA	Performance Assessment
pH	negative log of the hydrogen ion activity
pC_{H+}	negative log of the hydrogen ion concentration
Pu(III)	Plutonium in the +3 oxidation state, also written Pu^{3+}
Pu(IV)	Plutonium in the +4 oxidation state, also written Pu^{4+}
Pu(V)	Plutonium in the +5 oxidation state, also written PuO_2^+
Pu(VI)	Plutonium in the +6 oxidation state, also written PuO_2^{2+}
RPM	Revolutions per minute
SHE	Standard Hydrogen Electrode
SIT	Specific Ion Interaction Theory
SNL	Sandia National Laboratories
TDB	Thermodynamic Database
Th(IV)	Thorium in the +4 oxidation state, also written Th^{4+}
THEREDA	Thermodynamic Reference Database
TSD	Technical Support Documents
U(IV)	Uranium in the +4 oxidation state, also written U^{4+}

U(VI)	Uranium in the +6 oxidation state, also written UO_2^{2+}
WIPP	Waste Isolation Pilot Plant
XANES	X-ray Absorption Near-Edge Spectroscopy
XAS	X-ray Absorption Spectroscopy
Zr	Zirconium

Introduction

In the initial Compliance Certification Application (CCA) for the WIPP site, actinide redox was considered to be governed by reducing conditions and maintained by the anoxic atmosphere and iron dominated chemistry of the waste containers. In the CCA, plutonium was expected to exist in the +III or +IV oxidation state, while uranium was expected to be in the +IV and +VI oxidation state, and neptunium in the +IV and +V oxidation state (Weiner, et al. 1996). All other actinides, including thorium (+4), americium (+3), and curium (+3) were expected to be redox invariant over the range of conditions expected in the closed WIPP environment. These redox conditions have been maintained throughout the subsequent recertifications of the WIPP site (CRA-2004, CRA-2009, CRA-2014, CRA-2019).

In WIPP PA, the oxidation states of the actinides are governed by the parameter OXSTAT. OXSTAT is uniformly sampled between 0-1. If OXSTAT ≤ 0.5, the lower oxidation states [U(IV), Np(IV), and Pu(III)] control solubilities; if OXSTAT > 0.5, the higher oxidation states [U(VI), Np(V), Pu(IV)] control solubilities (CRA-2019, Appendix PA). This binary approach assumes that the redox of these three actinides are coupled, although that is not how they behave in nature. Under the most reducing aqueous conditions at pH 9.5, Pu(III), U(IV), and Np(IV) are the dominant solid and aqueous oxidation states. As E_h increases, first Pu(III) solids will oxidize to Pu(IV). There is a small range of E_h values where these Pu(IV) solids are in equilibrium with Pu(III) aqueous species. This is referred to as reductive dissolution. While the aqueous oxidation state is Pu(III), the solubility is controlled by the Pu(IV) solid. Further increase of E_h leads to Pu(IV) solids and aqueous species. U(IV) solids then oxidize to U(VI). Lastly, and at E_h values close to zero, which is the cutoff between oxidizing and reduced conditions, Np(IV) oxidizes to Np(V). This creates four distinct redox environments that could be expected to be present under the range of reducing conditions in the WIPP. A memo outlining this proposed change to the oxidation state model was accepted by DOE and implemented into the PA for CRA-2024.

Recently, the EPA has challenged the 50/50 assumption used in PA (Schramke, et al. 2020). Anoxic corrosion of the iron is expected to produce large quantities of hydrogen gas through the reaction:

$$Fe^0 + 2\,H_2O \rightarrow Fe(OH)_2 + H_2 \quad \text{(Formula 1)}$$

Further corrosion of the produced $Fe(OH)_2$ occurs by the Schikorr reaction:

$$3\,Fe(OH)_2 \rightarrow Fe_3O_4 + H_2 + 2\,H_2O \quad \text{(Formula 2)}$$

Giving the overall reaction:

$$3\,Fe^0 + 4\,H_2O \rightarrow Fe_3O_4 + 4\,H_2 \quad \text{(Formula 3)}$$

In PA calculations, this hydrogen gas can cause pressures in the WIPP to exceed 150 atm. In thermodynamic modeling, this hydrogen overpressure can cause the water reduction line to shift to lower E_h values than at atmospheric pressure. While this increases the stability field of Pu(III), there has been no direct evidence of hydrogen gas to reduce Pu(IV) to Pu(III) at

temperatures close to 25 °C. Due to this increase in the stability field of Pu(III), the EPA has asserted that the reduced oxidation states of the actinides will predominate under the expected WIPP conditions. In this context, it is helpful to discuss how the expected oxidation states were initially determined.

In the CCA, the expected oxidation states of the actinides were developed without any prior assumptions. The chemical environment was established as high ionic strength brine, at temperatures not to exceed 300 K. Reducing conditions in the repository are established through consumption of oxygen by aerobic microbial activity or corrosion of iron waste containers to produce hydrogen gas and Fe^{2+} (Brush 1990).

Thorium only exists as the +IV oxidation state in aqueous solution (Katz, et al. 1986). Uranium can exist in solution as the +III, +IV, +V, and +VI oxidation states (Hobart 1990; Clark, et al. 1995). However, in the natural environment, +IV and +VI are the dominate valence states. Any U(V) that would be produced would quickly disproportionate to U(IV) and U(VI) by the reaction (Arumungam and Burton 2021):

$$2\,U(V) \rightarrow U(IV) + U(VI) \qquad \text{(Formula 4)}$$

This reaction proceeds rapidly under the alkaline conditions expected in WIPP, but occurs slowly under acidic conditions (Selbin and Ortego 1969). The expected oxidation states for uranium are U(IV) and U(VI). Neptunium exists in the +IV, +V, and +VI oxidation states in the natural environment. Np(VI) is easily reduced by the organic compounds and iron found in WIPP waste, while Np(IV) and Np(V) are expected to be stable under the expected conditions. Plutonium can exist as the +III, +IV, +V, and +VI oxidation states. Pu(V) and Pu(VI) have been shown to be reduced by iron, and other reducing materials that are present in WIPP waste (Al Mahamid, et al. 1996; Reed, et al. 2003; Reed, et al. 2006). Pu(III) was observed in two WIPP brines at neutral pH, but was present below detection limits when pH > 9 (Felmy, et al. 1989). While Pu(IV) was expected to be the dominant oxidation state, Pu(III) was included in PA calculations, because its existence could not be ruled out (Weiner, et al. 1996).

Organic ligands present in WIPP waste also play a role in the chemistry and oxidation state of plutonium. EDTA and citrate are both knowns as strong chelators to plutonium in most oxidation states. Additionally, previous work has shown the ability of EDTA to rapidly reduce Pu(VI) to Pu(IV) (Reed, et al. 2003). This is also the expected behavior of citrate as it is also redox active. Oxalate and acetate, the other two prominent organic ligands found in WIPP waste, do not form strong complexes with Pu but their degradation can produce carbonate which forms strong complexes with Pu(III). The presence of these ligands can also impact the overall redox environment of the system they are present in. The presence and absence of these ligands, in concentrations expected during a DBR scenario, was used as a variable in these studies to determine their impact on the oxidation state distribution of Pu.

Plutonium behavior in brine is very dependent on the isotope used, brine chemistry, and the initial oxidation state of the plutonium. The main isotopes used for Pu laboratory studies are Pu-

238, Pu-239, and Pu-242. Pu-238 is very radioactive due to its short half-life (87.7 y). Pu-238 accounts for 30% of the activity of plutonium at repository closure, but quickly decays. Pu-239 is the predominant isotope found in WIPP bound waste by mass and has a half-life of 24,110 years. It accounts for 5.6% of Pu activity at repository closure, but 73% after 10,000 years due to its long half-life. Pu-242 is a minor (8.39% by activity) component of WIPP bound waste, but it is used in laboratory studies to minimize the impacts of radiolysis due to its longer half-life (375,000 years) (Van Soest 2018). Radiolysis occurs when high-energy alpha or beta particles or gamma rays produced through radioactive decay, interact with their surroundings. In water, this interaction leads the splitting of water molecules into hydrogen and hydroxide radicals. Through recombination, disproportionation, and radical reactions, this eventually leads to the production of hydrogen peroxide, oxygen gas, and hydrogen gas. However, in high ionic strength brines like those found in WIPP, the solute interactions play a role in the radiolysis chemistry. Previous studies of Pu-238 in 5 M NaCl brines, showed a large amount of hypochlorite ion forming in solution which led to the oxidation of Pu(IV) to Pu(VI) in a short time frame (56 days) (Büppelmann, et al. 1986). The WIPP chemical conceptual model assumes that the production of any species in solution by radiolysis will quickly react with the iron materials found in the waste containers (Hansen 2021).

Pourbaix diagrams give the speciation of an element as a function of pH and E_h. The speciation is set by the list of possible species included in the thermodynamic dataset used to calculate the diagrams. Commercially available datasets include the Nuclear Energy Agency Thermodynamic database (NEA-TDB), which contains log K values for a number of species related to the nuclear field. The Thermochimie database is jointly operated by the French, Belgian, and UK nuclear regulatory agencies, and contains log K values and ion interaction parameters calculated using the specific ion interaction theory (SIT) (Giffaut, et al. 2014; Grivé, et al. 2015). The Thermodynamic Reference Database (THEREDA) is funded by the Bundesgesellschaft Für Endlagerung (BGE, Federal Company for Radioactive Waste Disposal) in Germany, and contains log K values and Pitzer parameters for species related to the disposal of nuclear waste (Moog, et al. 2015). The WIPP database contains log K values and Pitzer parameters that have been internally calculated, as well as values that are found in other databases.

SIT and Pitzer equations are two commonly used theorems used to determine the extent of ion interactions in solutions at high ionic strengths. SIT is commonly used up to I = 3 M, whereas Pitzer has been used at high ionic strength values (I > 3 M). The use of SIT above I = 3 M results in deviations between the modeled speciation and solubility and the experimental results. While an SIT database contains a more complete set of species when compared to a Pitzer database, the use of SIT must be weighed against the deviations that may results in the calculations. If sufficient Pitzer parameterization is available, it should be the model used for WIPP applications.

Experimental Details

All experimental work was done according to test plan LCO-ACP-25, rev. 0, "Effects of Radiolysis, Organic Complexation, and Redox Conditions on the Speciation and Oxidation State Distribution of Pu(III/IV)." 90% strength Generic Weep Brine (GWB), pC_H 9, and pC_H 10 brines were prepared according to procedure LCO-EXP-001, rev. 3, Brine Preparation. The composition of these brines are given in Tables 1 and 2. 30 mL polypropylene bottles were conditioned with brine solutions for 2 weeks before experiments began. All brine preparations, final plutonium stock preparations, experimental setup, and sampling was conducted in a nitrogen atmosphere glovebox. Oxygen partial pressure was kept below 10 ppm throughout the experiments. Samples were doubly contained in sealed vessels to prevent any exposure to oxygen and prevent sample evaporation. All pipettes used during brine preparation, stock solution generation, and sampling were checked for compliance with the stated volumes according to procedure LCO-ACP-EXP-004, rev. 4, Pipet Performance Checks.

Table 1. Composition of WIPP brine solutions used in plutonium solubility experiments

Chemical Name	Supplier	Lot #	Mass added (g) 90% GWB	Mass added (g) 90% pC_{H+} 9	Mass added (g) 90% pC_{H+} 10
$Na_2B_4O_7 \cdot 10H_2O$	Acros Organics	A013620101	13.2572	13.3471	0.9604
$MgCl_2 \cdot 6H_2O$	Fisher Scientific	168170	183.0077	188.7367	21.4098
$CaCl_2 \cdot 2H_2O$	Fisher Scientific	040676	1.862	1.7806	1.7656
LiCl	Fisher Scientific	015295	0.1587	0.1452	0.1376
KCl	Fisher Scientific	103665	30.9144	30.727	30.1995
NaBr	Fisher Scientific	010543	2.4125	2.1736	2.1693
Na_2SO_4	Fisher Scientific	138245	22.3345	22.5105	21.6168
NaCl	Fisher Scientific	168160	149.9228	151.7452	243.7894

Table 2. Concentrations of WIPP brine components used in plutonium solubility experiments

Ion	90% GWB (M)	90% pC_{H+} 9 (M)	90% pC_{H+} 10 (M)
Li^+	0.0037	0.0034	0.0032
Na^+	2.9729	2.9697	4.4996
Mg^{2+}	0.9002	0.9284	0.1053
K^+	0.4147	0.4122	0.4051
Ca^{2+}	0.0127	0.0121	0.0120

Cl^-	4.8095	4.8931	4.8146
SO_4^{2-}	0.1572	0.1585	0.1522
Br^-	0.0234	0.0211	0.0211
BO_4^-	0.1390	0.1400	0.0101

Table 3 includes a description of the experimental variables including plutonium isotope, pC_{H+}, presence or absence of WIPP organics, and iron phase used. Both Pu-239 and Pu-242 were used in these experiments. Both isotopes were procured from Oak Ridge National Laboratory and received as a high-fired oxide. Preparations for stock solutions of each isotope follow the same procedure. Pu(III) was prepared by fuming high-fired PuO_2 with concentrated hydrobromic acid (HBr) (Aldrich, lot# 15826TA) at 120 °C. The residual solid was dissolved in high purity water to produce a Pu(III) stock solution. The oxidation state purity of this solution was confirmed by UV-vis spectroscopy (Figure 1). Pu(IV) was prepared through the addition of 6 M nitric acid (HNO_3) (Fisher Scientific, lot# 4217070) to the Pu(III) solid from the previous preparation and taken to dryness. This solid was resuspended in 1 M HCl to produce a Pu(IV) stock solution.

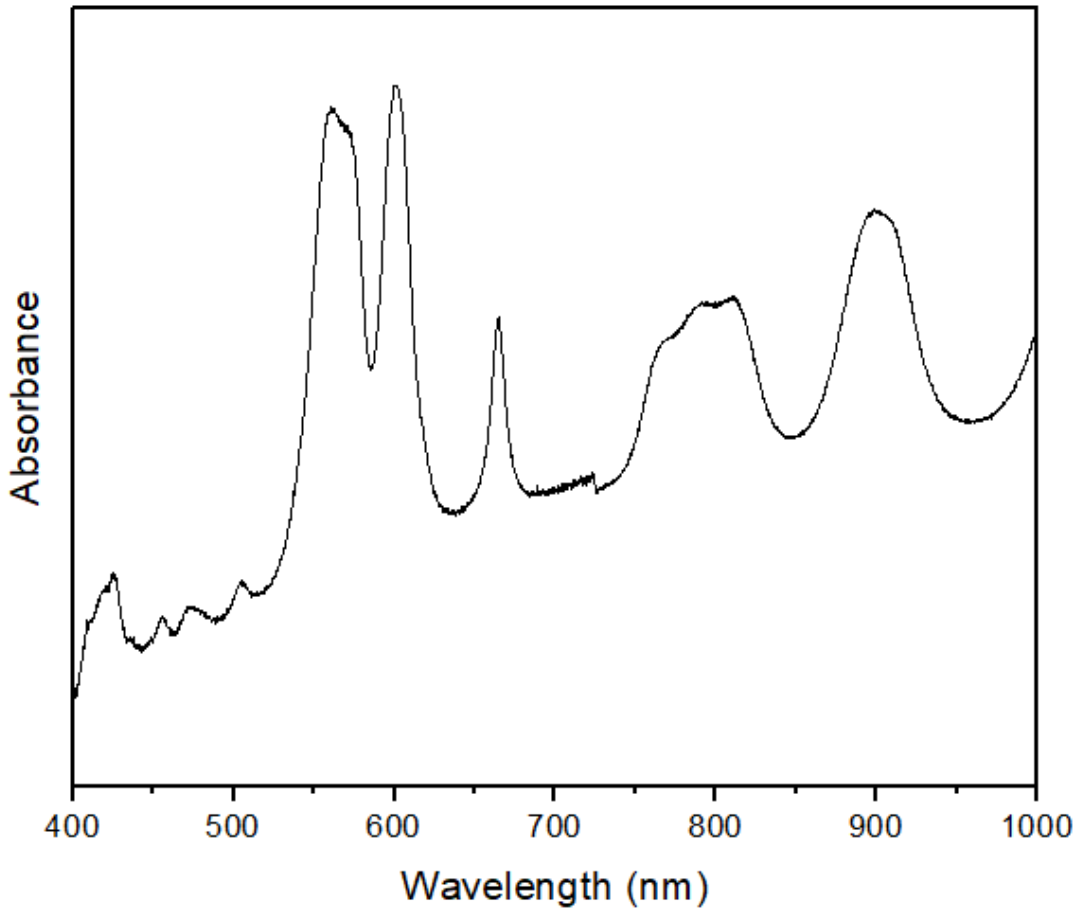

Figure 1. UV-vis spectroscopy of Pu(III) starting material in high purity water.

$Pu(OH)_3$ was prepared by adding an aliquot of the Pu(III) stock solution to the previously conditioned polypropylene bottles. An equal volume of 50% carbonate free sodium hydroxide (NaOH) (Acros Organics, lot# A0277324) was added to precipitate the blue $Pu(OH)_3$ solid.

$Pu(OH)_4$ was prepared by adding an aliquot of the Pu(IV) stock solution to the previously conditioned polypropylene bottles. An equal volume of 50% carbonate free NaOH was added to precipitate the yellow $Pu(OH)_4$ solid.

20 mL of the appropriate brine solution was added to each plutonium solid. Stock solutions of EDTA ($Na_2EDTA{\cdot}2H_2O$, Sigma-Aldrich, lot# SLI3525134), citrate (citric acid anhydrous, Fluka, lot# 447332/1), acetate (acetic acid, Acros Organics, lot# A0258955), and oxalate (Na_2oxalate, Aldrich, lot# 068040A) were prepared and added to individual solutions to prepare concentrations of the organic ligands equivalent to the 1x dilution concentrations expected in a direct brine release (DBR) (Van Soest 2018). Commercially available iron powder (Aldrich, lot# 09216EB) or magnetite (Fe_3O_4) (Aldrich, lot# 14201HE) were added to create reducing environments.

pH measurements were taken with a Ross semi-micro combination electrode, and an Orion 3 Star meter. The electrode was calibrated with pH 4 (AC-04-15), 7 (AC-07-15), and 10 (AC-10-15) buffers according to procedure ACP-EXP-002, rev. 2, pH Electrode/Meter Calibration. The calibration was then confirmed by occasional checks of the pH 10 buffer solution. pH adjustments of the solutions were performed through the addition of 50% carbonate free NaOH and 6 M HCl. Corrections of measured pH values to pC_{H+} were done according to established procedure (Borkowski et al. 2011).

Oxidation-reduction potentials (ORP) measurements were taken with a platinum electrode filled with a 3 M KCl solution saturated with silver chloride, and Orion 3 Star meter. The electrode was calibrated with Zobell's solution to +225 mV at 25 °C. Error associated with ORP measurements are ± 12 mV, as determined by periodic checks of the calibration solution. Corrections from redox potential to E_h were done by adding the Ag/AgCl redox potential from the meter reading (US EPA 2013).

Inductively coupled plasma mass spectroscopy measurements were used to calculate plutonium concentrations in the solutions according to procedure LCO-EXP-011, rev. 5, Inductively Coupled Plasma Mass Spectrometry (ICP-MS). A 500 µL sample from each experiment was centrifuged through a 10K Pall nanosep filter in an Eppendorf Minispin centrifuge at 13K RPM for 30 minutes. 100 µL of the filtrate was diluted into 900 µL 2% HNO_3 to produce a 1:10 dilution. 100 µL of this 1:10 dilution was then added to 1700 µL of a 2% HNO_3 solution containing 300 ppb In internal standard (High Purity Standard, lot# 2013216) to produce a final dilution of 1:180.

X-ray absorption spectroscopy (XANES) samples were prepared by removing solid from each experiment, filtering it through a 100K Amicon filter using an Eppendorf Minispin centrifuge at 13K RPM for 30 minutes, and diluting the solid in boron nitride. XANES spectra were collected at the 10-BM beamline at the Advanced Photon Source (APS). The Pu L_3-edge spectra were

collected in fluorescence mode using a 4 element Vortex detector and calibrated with Zr foil (E_0 = 17995.8 eV) collected in-line with the Pu spectra. Spectra were calibrated and normalized using the Athena software program. Linear combination fitting was performed with Athena using Pu(III) [$Pu(OH)_3$] and Pu(IV) [PuO_2] spectra to fit the experimental spectra (Ravel and Newville 2010).

Table 3. Experimental matrix for plutonium oxidation state studies.

Sample ID	Pu isotope	Initial Oxidation State	Organics Present	Iron Phase
Pu239_3_pH8_Fe0_1,2	239	+3	No	Fe^0
Pu239_3_pH9_Fe0_1,2	239	+3	No	Fe^0
Pu239_3_pH10_Fe0_1,2	239	+3	No	Fe^0
Pu239_3_pH8_Fe(II/III)_1,2	239	+3	No	Fe_3O_4
Pu239_3_pH9_ Fe(II/III)_1,2	239	+3	No	Fe_3O_4
Pu239_3_pH10_ Fe(II/III)_1,2	239	+3	No	Fe_3O_4
Pu239_3_pH8_org_Fe0_1,2	239	+3	Yes	Fe^0
Pu239_3_pH9_org_Fe0_1,2	239	+3	Yes	Fe^0
Pu239_3_pH10_org_Fe0_1,2	239	+3	Yes	Fe^0
Pu239_3_pH8_org_Fe(II/III)_1,2	239	+3	Yes	Fe_3O_4
Pu239_3_pH9_org_Fe(II/III)_1,2	239	+3	Yes	Fe_3O_4
Pu239_3_pH10_org_Fe(II/III)_1,2	239	+3	Yes	Fe_3O_4
Pu239_3_pH8_1,2	239	+3	No	-
Pu239_3_pH9_1,2	239	+3	No	-
Pu239_3_pH10_1,2	239	+3	No	-
Pu242_3_FepH9	242	+3	No	Fe^0
Pu242_3_FepH10	242	+3	No	Fe^0
Pu242_3_pH9	242	+3	No	-
Pu242_3_pH10	242	+3	No	-
Pu242_4_pH8_1,2	242	+4	No	-
Pu242_4_pH9_1,2	242	+4	No	-
Pu242_4_pH10_1,2	242	+4	No	-

Results and Discussion

The brine chemistry of the WIPP is bracketed by Generic Weep Brine (GWB) and Energy Research and Development Administration Well 6 (ERDA-6) brines, which are typical of the Salado formation the WIPP lies in and the underlying Castille formation, respectively. These brines are primarily NaCl, with minor amounts of Li^+, Na^+, Ca^{2+}, K^+, BO_4^-, Br^-, and SO_4^{2-}. The major difference between GWB and EDRA chemistry is in the amount of dissolved Mg^{2+} present in the brines. GWB has a maximum [Mg^{2+}] of 1 M, while ERDA-6 has a maximum [Mg^{2+}] of 19 mM. Prepared GWB has a pC_{H+} around 7. As the calculated pC_{H+} of reacted brines is around 9.5, it is helpful to use a stable brine formulation at that pH value to minimize precipitation of any brine components while performing pH adjustments. These pC_{H+} specific brines were developed to

study the effects of brine chemistry at a range of pC_{H+} values relevant to the WIPP system. In experiments concerning actinide solubility and speciation, it is often useful to use these brines in a 90% saturation state to prevent precipitation of any brine components.

The pC_{H+} of the prepared WIPP brines are stable. Over the course of 205 days, pC_{H+} in most samples was within half a pH unit of the initial pC_{H+}. Some of the samples had changes in pC_{H+} that were over 1 pH unit higher than the initial value. This could be due to the build-up of radiolysis products in experiments containing partially oxidized iron. Table 4 shows the shift in pC_{H+} as a function of time over the duration of these solubility experiments.

The solubility of plutonium under these conditions ranges over five orders of magnitude (Figure 2). The spread in solubility is highest at pC_{H+} = 9. In general, the solubility increases in the presence of organic ligands, and is also higher in the presence of more oxidized forms of iron.

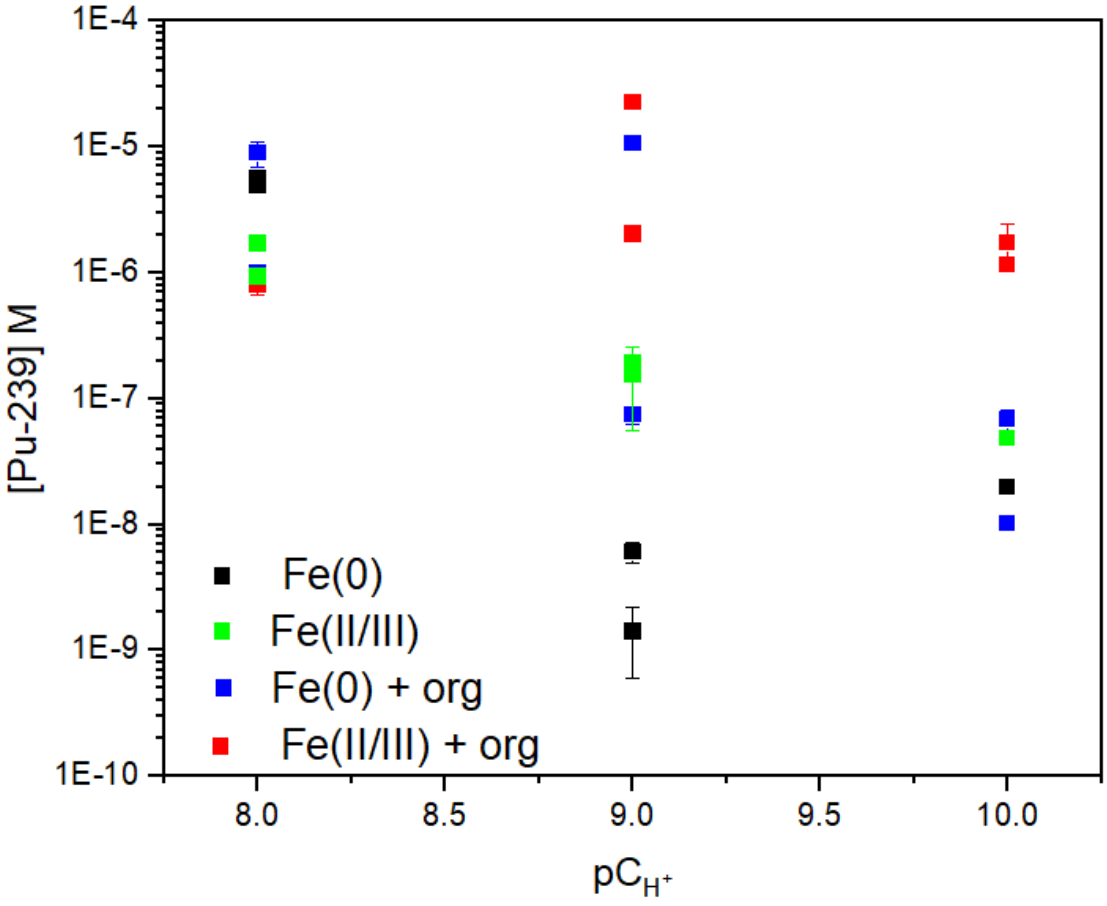

Figure 2. Solubility of plutonium as a function of pC_{H+}.

Table 4. pC_{H+} values as a function of time in Pu solubility experiments. The range of values over 205 days is given in the last column.

	Days				
Sample ID	21	28	103	205	Δ pC_{H+}
Pu239_3_pH8_org_Fe23_1	7.87	7.99	9.05	9.03	1.18
Pu239_3_pH8_org_Fe23_2	7.96	8	8.56	8.59	0.63
Pu239_3_pH9_org_Fe23_1	8.92	9.05	9.36	9.28	0.44
Pu239_3_pH9_org_Fe23_2	8.98	9.07	9.3	9.24	0.32
Pu239_3_pH10_org_Fe23_1	10.05	10.04	9.45	9.82	0.6
Pu239_3_pH10_org_Fe23_2	10.06	10.1	9.74	10.01	0.36
Pu239_3_pH8_Fe23_1	8.04	8.05	8.12	8.24	0.2
Pu239_3_pH8_Fe23_2	7.95	8.09	8.13	8.35	0.4
Pu239_3_pH9_Fe23_1	8.97	9.13	9.13	9.34	0.37
Pu239_3_pH9_Fe23_2	9.01	9.07	9.14	9.25	0.24
Pu239_3_pH10_Fe23_1	9.96	10.12	9.7	9.83	0.42
Pu239_3_pH10_Fe23_2	9.94	10.01	9.57	9.86	0.44
Pu239_3_ pH8_Fe0_1	8.05	8.01	8.97	8.96	0.96
Pu239_3_pH8_Fe0_2	8.01	8.03	8.51	8.53	0.52
Pu239_3_pH9_Fe0_1	9.05	9	9.23	9.21	0.23
Pu239_3_pH9_Fe0_2	9.02	8.9	9.2	9.16	0.3
Pu239_3_pH10_Fe0_1	10.06	9.89	9.34	9.74	0.72
Pu239_3_pH10_Fe0_2	10	9.93	9.66	9.75	0.34
Pu239_3_org_Fe0_pH8_1	8.06	8.05	8.25	8.28	0.23
Pu239_3_org_Fe0_pH8_2	8.06	7.93	8.27	8.3	0.37
Pu239_3_org_Fe0_pH9_1	9.08	9.05	9.21	9.26	0.21
Pu239_3_org_Fe0_pH9_2	9.06	9.08	9.17	9.18	0.12
Pu239_3_org_Fe0_pH10_1	10.18	10.11	9.94	9.9	0.28
Pu239_3_org_Fe0_pH10_2	10.14	10.03	9.95	9.91	0.23

The iron chemistry of the WIPP is crucial to setting the E_h of the repository. All scenarios including WIPP having a reducing environment (E_h < 0 mV) due to the large amount of iron present in the waste and packaging materials. The iron has multiple possible fates. The first is conversion to FeS through reaction of iron with H_2S gas which is the byproduct of sulfate reducing microbial activity that could occur in the closed repository. Another possibility is the formation of magnetite (Fe_3O_4) through continued reaction with oxygen gas and corrosion from intruding brine. FeS is expected to be thermodynamically stable under very reducing E_h conditions and would convert to magnetite under milder conditions. If FeS formation is

suppressed, magnetite is stable over a wide range of E_h values, including those at the water reduction line and under oxidizing conditions ($E_h > 0$) (Figure 3).

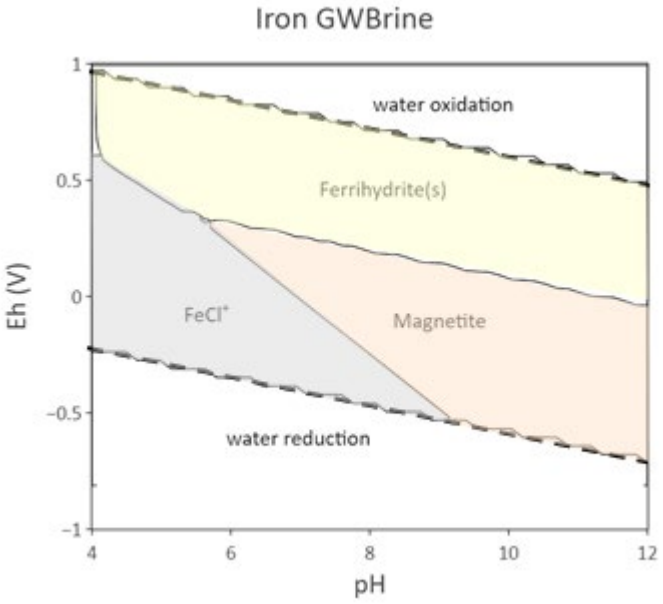

Figure 3. Iron Pourbaix diagram in GWB. FeS formation is not allowed.

The plutonium speciation is more complex than the iron chemistry. In the WIPP pH range (8 < pH < 10), there are three regions of the Pourbaix diagram that are important to discuss (Figure 4). The first is the strongly reducing conditions close to the water reduction line. This area is dominated by $Pu(OH)_3$ solids in equilibrium with dissolved Pu(III) species, as the solubility of Pu is very low in alkaline, high ionic strength conditions. As the E_h increases, Pu(III) solids oxidized to Pu(IV), but still maintaining the Pu(III) oxidation state in dissolved species. This process is referred to as reductive dissolution, as the Pu(IV) solid will reduce as it dissolves to produce Pu(III). Although Pu(III) is present in solution, the solubility is still governed by the Pu(IV) solid.

The ORP and corrected E_h values for the Pu solubility experiments are given in Table 5. Under the experimental conditions investigated in this report, only the presence of Fe(0) maintained reducing conditions. All experiments that contained Fe_3O_4 resulted in oxidizing conditions. While there is a vast range of redox conditions over these experiments, they are all firmly in the stability field of PuO_2. As the WIPP conceptual model assumes reaction of radiolytic products with the iron metal in the repository, the ability for partially oxidizes iron phases to react with this products is of interest to the project. The E_h measurements correlate somewhat to the solubility measurements, as higher solubilities are observed at higher E_h values. Under increased H_2 pressures, the high E_h boundary between Pu(III) and Pu(IV) does not change significantly, which means that unless WIPP conditions are very close to the water reduction potential, Pu(III) should not be thermodynamically stable (Figure 5).

Table 5. ORP measurements, and E_h corrections for Pu solubility experiments. ORP measurements are corrected to E_h by adding the half-cell potential of Ag/AgCl reference (+209 mV at 25 °C).

Sample	ORP (mV)	E_h (mV)
Pu239_3_pH8_org_Fe23_1	190.7	399.7
Pu239_3_pH8_org_Fe23_2	95.7	304.7
Pu239_3_pH9_org_Fe23_1	102.1	311.1
Pu239_3_pH9_org_Fe23_1	119.6	328.6
Pu239_3_pH10_org_Fe23_1	135.5	344.5
Pu239_3_pH10_org_Fe23_2	152.7	361.7
Pu239_3_org_Fe0_pH8_1	-378.4	-169.4
Pu239_3_org_Fe0_pH8_2	-391.2	-182.2
Pu239_3_org_Fe0_pH9_1	-342.6	-133.6
Pu239_3_org_Fe0_pH9_2	-203.9	5.1
Pu239_3_org_Fe0_pH10_1	-416.7	-207.7
Pu239_3_org_Fe0_pH10_2	80.5	289.5
Pu239_3_ pH8_Fe0_1	-386.1	-177.1
Pu239_3_pH8_Fe0_2	-455.8	-246.8
Pu239_3_pH9_Fe0_1	-405.4	-196.4
Pu239_3_pH9_Fe0_2	-425.2	-216.2
Pu239_3_pH10_Fe0_1	-447.3	-238.3
Pu239_3_pH10_Fe0_2	-447.5	-238.5
Pu242_4_pH8_1	216.5	425.5
Pu242_4_pH8_2	214.7	423.7
Pu242_4_pH9_1	204.5	413.5
Pu242_4_pH9_2	148.1	357.1
Pu242_4_pH10_1	182.5	391.5
Pu242_4_pH10_2	147.3	356.3
Pu239_3_pH8_Fe23_1	197.3	406.3
Pu239_3_pH8_Fe23_2	149.3	358.3
Pu239_3_pH9_Fe23_1	184.6	393.6
Pu239_3_pH9_Fe23_2	200.3	409.3
Pu239_3_pH10_Fe23_1	195.9	404.9
Pu239_3_pH10_Fe23_2	199.1	408.1

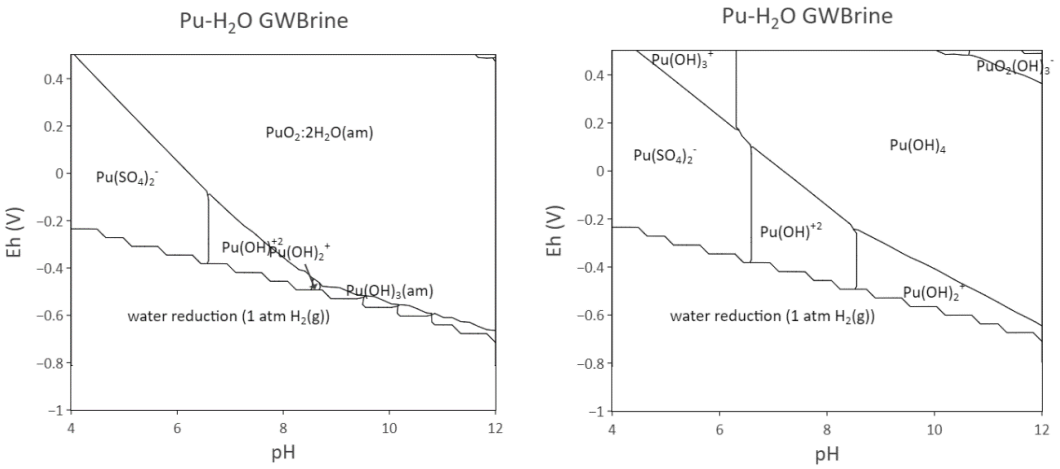

Figure 4. Comparison of Pu speciation left) including solids, and right) only aqueous species under 1 atm H_2 overpressure. Diagrams were calculated using the Thermochimie SIT database.

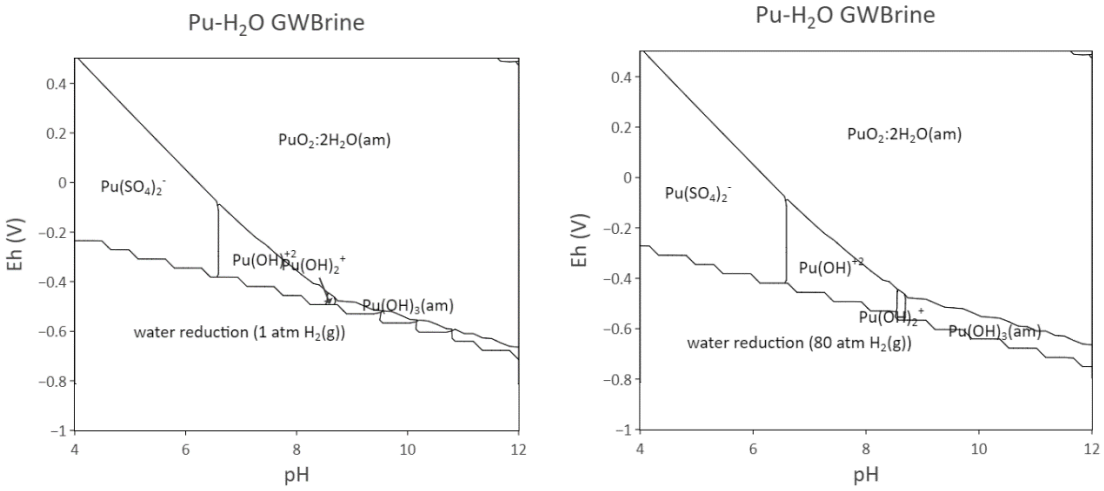

Figure 5. Pourbaix diagrams of plutonium ([Pu] = 1.2×10^{-7} M) solids in GWB under a) 1 atm and b) 80 atm H_2 overpressures. Diagrams were calculated using the Thermochimie SIT database.

With the E_h measurements being in a range that would indicate oxidation of the initial Pu(III) starting material to Pu(IV), direct measurement of the oxidation state is useful to obtain to see the correlation of the two measurements. X-ray absorption spectroscopy is a useful technique for the identification of oxidation states for a variety of elements. For plutonium, the L_3-edge is widely used to identify its oxidation state (Conradson, et al. 2011). In Pu L_3-edge XANES, X-rays cause the excitation of a 2p electron out of the atom, this is then followed by relaxation of an electron into the hole that was formed, which causes the emission of a photon as fluorescence. Slight changes in the onset energy of this absorption process can be correlated to the oxidation state. As Pu^{4+} has less valence electrons than Pu^{3+}, the excitation of the 2p electron takes slightly more energy. The Pu L_3-edge XANES spectra contain no pre-edge features that may be able to identify the oxidation state or coordination geometry. The spectra contain just one absorption feature which is called a white line. Another distinctive feature of Pu L_3-edge XANES is the

presence of a peak near the absorption edge for Pu(V) and Pu(VI) species which is indicative of the plutonyl functional group (Figure 6). This makes the speciation between Pu(III/IV) and Pu(V/VI) very straightforward. Due to the difference in the onset energy and white line position of Pu(III) and Pu(IV) species, a linear combination fit using one spectrum of each of these oxidation states can be used to fit the oxidation state of an unknown solid. Linear combination fitting uses the formula:

$$1 - x(A) + x(B) = C \quad \text{(Formula 5)}$$

Where A and B are the two component spectra, C is the composite spectra and x is a fitting variable. As changes in the coordination environment can impact both the white line position and onset energy, the component spectra should be similar in composition to the unknown. The species chosen for the linear combination fits for the plutonium spectra were $Pu(OH)_3$ and $PuO_2{\cdot}xH_2O$, as these are the expected solubility controlling phases for each oxidation state under WIPP conditions.

An example LCF result is presented in Figure 7, along with the component spectra and the residual of the fit. The fit range was chosen to encompass both the onset energy as well as the entire absorption feature. The results of the fits as a percentage of Pu(III) and Pu(IV) character of each sample is given in Table 6. In general, the samples are primarily Pu(IV) with small amounts of Pu(III) character.

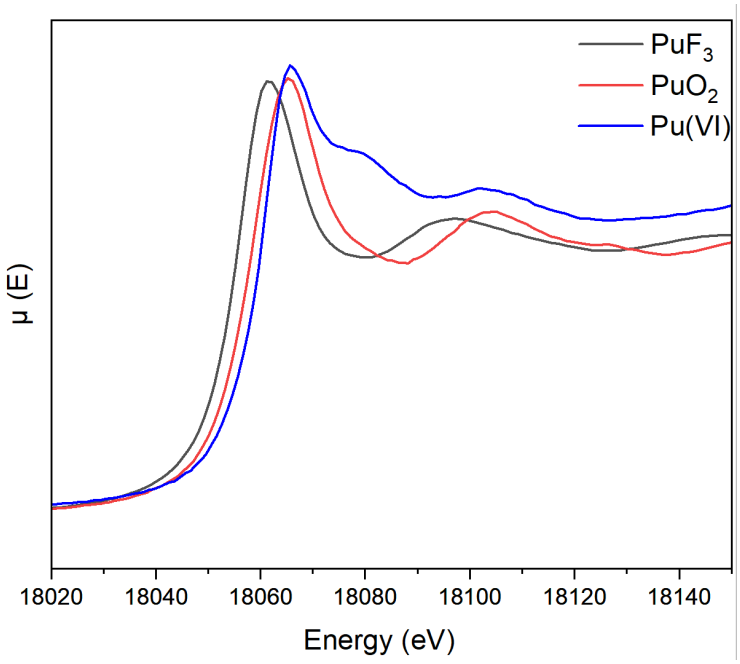

Figure 6. XANES spectra of Pu(III), Pu(IV), and Pu(VI) solids showing the difference in onset energy, white line position, and post-edge features.

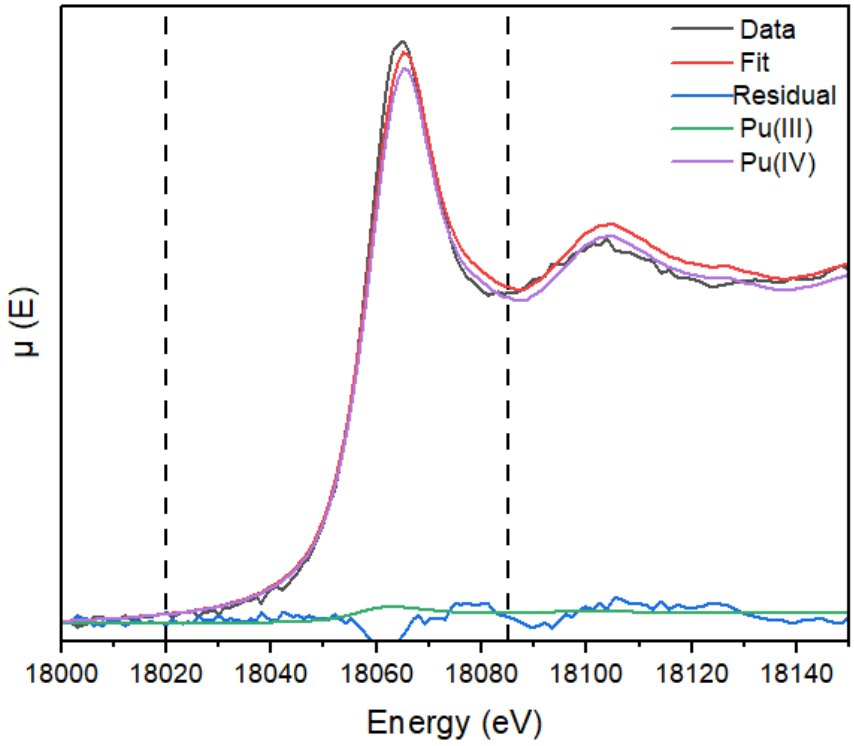

Figure 7. LCF example result showing character of Pu(III) and Pu(IV) spectra. The black dashed lines indicate the range used for the fit.

Table 6. LCF analysis of Pu(III)/Pu(IV) XANES spectra. Error is ± 10%.

Sample ID	% Pu 3	% Pu 4
Pu239_3_pH8_1	3.66	96.34
Pu239_3_pH9_1	1.09	98.91
Pu239_3_pH10_1	3.19	96.81
Pu242_pH9	5.12	94.88
Pu242_FepH9	4.67	95.33
Pu239_3_Fe0_pH8_2	13.15	86.85
Pu239_3_Fe0_pH9_2	21.25	78.75
Pu239_3_Fe0_pH10_2	2.91	97.09
Pu239_3_Fe23_pH8	3.29	96.71
Pu239_3_Fe23_pH9	1.77	98.23
Pu239_3_Fe23_pH10_2	3.66	96.34
Pu239_3_Fe23_org_pH8_1	3.85	96.15
Pu239_3_Fe23_org_pH9_1	2.91	97.09
Pu239_3_Fe23_org_pH10_1	1.96	98.04
Pu242_pH10	5.57	94.43
Pu242_FepH10	4.03	95.97

Conclusion

Strongly reducing conditions were maintained though the addition of iron to Pu-239 solubility experiments in the presence and absence of WIPP relevant organic ligands. These reducing conditions were not strong enough to maintain Pu(III) stability. In the presence of Fe_3O_4, the solutions become oxidizing, likely due to the buildup of radiolysis products in the reaction vessels. While these conditions are oxidizing, they are still within the stability field of Pu(IV) solids. Pu(IV) solids are confirmed to be the dominant oxidation state under all experimental conditions through LCF of XANES spectra. A formal summary of the expected oxidation states under WIPP conditions will be generated in a parameter update report to parameterize the oxidation state model in WIPP PA calculations for CRA-2024.